Report

on

.

Evaluation of Compliance of Palmtop CASIO Computer, "Cassiopeia", model A-11 with an AirCard modem with the FCC 96-326 Guidelines for Evaluating Environmental Effects of Radiofrequency Radiation

Prepared for:

Sierra Wireless, Inc.

13151 Vanier Place, # 260

Richmond, BC

Canada, V6V 2J2

Prepared by:

M.A. Stuchly, Ph.D., P.Eng., Professor

M. Okoniewski, Ph.D., Adjunct Assist. Professor

Department of Electrical and Computer Engineering,

University of Victoria, Victoria, BC

July, 1998

Introduction

This report provides results of a numerical evaluation of the maximum specific absorption rate (SAR) produced in the human tissue by a palmtop computer with modem, FCC ID: BBQZX305-1, here-upon called the device under test or the test device. The evaluation is performed for the worst case configurations of the test device and the user's head with respect to the FCC 96-326 Guidelines. The purpose of the evaluation is to establish compliance with the Federal Communication Commission FCC 96-326 Guidelines for Evaluating the Environmental Effects of Radiofrequency Radiation, ET Docket No. 93-62, adopted August 1, 1996. The information submitted shows that even under the worst case conditions the device under test meets FCC requirements, specifically:

- whole-body averaged SAR not exceeding 0.08 W/kg,
- SAR averaged over 1 gram of tissue not exceeding 1.6 W/kg.

The format of the information provided follows the list of technical items for the numerical SAR evaluation outlined in Supplement C (Edition 97-01) to OET Bulletin 65 (Edition 97-01).

Test Device Setup and System Uncertainties

General Information

- FCC ID: BBQZX305-1
- device category: portable,
- RF exposure environment: uncontrolled,
- test method: computation with the finite difference time domain (FDTD) method,
- affirmative statements: the device under test complies with FCC adopted limits:

"For the device user, under the worst-case realistic exposure condition, 1g averaged SAR does not exceed the prescribed value of 1.6 W/kg, and the whole-body average SAR does not exceed 0.08 W/kg. These limits are not exceeded for the antenna either extended or retracted. It is unrealistic to expect that a bystander can place his/her head closer to the antenna than the user, while the device is in use".

Antenna Description

- antenna type: PCB whip with a metallic cup on top and lumped elements at the input,
- antenna location on device: plugged into the AirCard located on the right-hand side of the keyboard,
- antenna dimensions: extended: length 107 mm, and retracted length 63 mm; diameter top 1.8 mm, bottom copper printed on dielectric,
- antenna configurations modeled: retracted and extended, vertical.

Test Signal and Output Power

- test signal: CW, no time averaging used, frequency 837 MHz (Gaussian pulse used in computation and Fourier transform to get CW results),
- output power: maximum 600 mW (specified by the manufacturer).

Test Position and Conditions

- head position: the model of the human head is placed as close to the device screen as judged possible for an extremely shortsighted person, who wants to read the text on the screen. Under normal circumstances, the usual and comfortable work position is much further away from the computer screen. The head is slightly tilted, as illustrated in Fig.1. Hands are not included, as their absence results in higher power deposition in the head;

- device position: the computer screen is tilted 140 degrees with respect to the keyboard, this is a position that appears to be "natural", and in which the external surfaces (associated with hinges) of the keyboard and the screen are aligned;
- antenna position: plugged into the AirCard in the vertical position; two positions: antenna retracted and extended.

Computation Uncertainty

- description of computational uncertainties: there are several potential sources of error. The estimated uncertainty associated with them is:

Anatomical model of the head; anatomy differences	10 %
Dielectric properties of tissues	5 %
Antenna modeling	3 %
Device modeling	3 %
FDTD: staircasing, dielectric properties averaging	1 %
SAR averaging	1 %

- estimated total uncertainty 12 %

Information for SAR Computation

Basic FDTD Parameter Description

- Domain size: 388 x 264 x 296 mm without PMLs (orientation of the coordinates shown in Fig. 1), cell size 2 x 2 x 2 mm^3, time step 3.81 ps
- ABC type: PML, 7 layers, parabolic, reflection -40 dB.
- Source excitation: Gaussian pulse centered at 840 MHz, Δf = 300 MHz
- Total time steps: 3000

- Method used to determine steady state: the following observations and criteria are used: (i) electric field probes are placed in the following locations: in tissue close to the expected peak SAR (determined after a preliminary run), close to the antenna feed and in a corner of the computational domain (close to the PML); the simulation is stopped when the field changes are less than 0.2 %, (ii) the energy at the antenna input is less than 0.1 % of the applied pulse energy, and (iii) the antenna input impedance changes are below 2 %. All the conditions have to be satisfied to deem the computation valid.
- Special FDTD techniques used:

(i) conformal metals algorithm used to model exactly the metals of the tilted screen part of the computer and the dipole radius in the benchmark problem (see reference Anderson et al., 1996),

(ii) conformal dielectrics algorithm used to model various tissues of the human head,

(iii) antenna lumped elements (standard representation, as in reference Taflove, 1995).

- Benchmark of FDTD technique & results

To demonstrate validity of our FDTD code, as a benchmark problem we computed the far field radiation pattern and input impedance of a dipole in free space. The dipole length was 17.01 cm, and radius 0.039 cm. The mesh used was dx=dy=0.85 cm and dz=0.81 cm. The results obtained for the FDTD were compared with those from the method of moments, the NEC code (the analytical solution is available only for infinitely thin wires). Figure 2 shows the radiation patterns in the yz plane (E plane) at the resonant frequency. The two patterns are indistinguishable. A more critical evaluation can be made using the input impedance, as shown in Fig. 3. At the resonant frequency the error in the radiation resistance is about 0.5 %.

Tissue Model Description

- Source of head model: CT and MRI scans and segmentation performed at Medical School of the Yale University (see reference Zubal et al., 1994), and improved in our laboratory by application of the skin, refinements to the ear and correction of smaller model imperfections.
- Model resolution: 1.1 x 1.1 x 1.4 mm down to the lower jaw, and 3.6 mm below the lower jaw.
- Model shape and complexity: accurate shape for an average male of 1.76 m high and 75 kg mass, over 30 tissue types segmented, extensive visual examination and editing performed to ensure correct anatomical representation, an anatomist-medical doctor consulted during improvements at the University of Victoria.
- Tissue types and dielectric properties: data used in this test are given in Table 1.
- Benchmark description & results

To demonstrate our FDTD code performance for modeling of lossy dielectrics and computation of 1g (cube) peak SAR a benchmark problem is computed, that comprises a resonant dipole at a close distance to a glass sphere containing material whose dielectric properties are the same as the brain tissue. The dipole length is 168 mm and diameter is 3.6 mm. The dipole is separated 5 mm from the glass sphere. The outer sphere diameter is 223 mm and the glass thickness is 5 mm. The dielectric properties are as follows: for glass $\varepsilon_r = 4$ and $\sigma = 0$, and for the brain $\varepsilon_r = 44$ and $\sigma = 0.90$ S/m. The frequency of computations is 840 MHz. The computational domain used for this benchmark is 260 mm x 247 mm x 247 mm. Domain termination is PML (7, P, - 40 dB).

Grid is: (i) around the dipole center: x = y = z = 1 mm, 5 grids in each direction;

(ii) graded mesh with expansion approx. 1:1.25 till x = y = z = 2 mm;

(iii) constant x = y = z = 2 mm maintained for 17 grids;

(iv) further mesh expansion with 1:1.25.

Table 1. Dielectric properties of some tissues used in the evaluation, frequency 836 MHz

Tissue	**ε'**	***s* (S/m)**	**ρ(kg/m^3)**

skin	41.2	0.84	1040
skull	12.5	0.13	1850
spinal cord	32.7	0.56	1040
spine	12.5	0.13	1850
brain - white	39.1	0.57	1030
brain - gray matter	53.0	0.91	1030
jaw bone	12.5	0.13	1850
muscle	56	0.92	1040
parotid gland	57.6	1.24	1050
lacrimal glands	57.6	1.24	1050
spinal canal	68.8	2.38	1010
tongue	55.5	0.91	1050
hard palate	42.9	0.75	1100
nasal septum	35	0.6	1100
fat	11.4	0.10	920
blood	61.5	1.51	1060
CSF	68.8	2.38	1010
eye - sclera	55.5	1.14	1020
eye - humor	55.5	1.14	1010
lens	46.7	0.77	1100
bone marrow	42	0.8	1060
cartilage	42.9	0.75	1100
pituitary gland	57.6	1.24	1070
ear bones	42.9	0.75	1810

Special algorithms used are:

(i) conformal metals algorithm used to model exactly the diameter of the dipoles (see reference Anderson et al., 1996),

(ii) conformal dielectrics algorithm used to model the sphere, and

(iii) automatic computation of mass-averaged SAR algorithm, Caputa et al., 1998). Excitation is: Gausian pulse, centered at 840 MHz and f = 300 MHz, 50 source; impedance computed from the electric field in the dipole gap and the magnetic fields around the contour centered on the gap with correction for t/2.

Summary results are given in Table 2, and Fig. 4.

Table 2. Impedance and voxel peak SAR, 1 g SAR and 10 g SAR, all values normalized to 1 W dipole output power and for f = 840 MHz.

Impedance(Ω)	SAR (W/kg) per 1 W		
	Voxel (peak)	1 g (peak)	10 g (peak)
48.5 + j 5.75	17.33	12.13	7.6

Test Device Model Description

- The device under test model consists of the following main components: keyboard bottom part, the screen part, modem (AirCard), battery and antenna. The model of the keyboard consists of a metallized PCB in electrical contact with a few metallic boxes representing other metallic structures inside this part of the palmtop, these metallic parts are covered with a dielectric material. The relative dielectric constant is 3 and the material is assumed loss-less. The keyboard keys are modeled as a loss-less dielectric with a dielectric constant of 2 (to account for the combination of plastic and air which actually constitute the keys). The computer screen part is similarly modeled as a metallic PCB imbedded in the same dielectric as the keyboard part, but with the screen represented by a low-loss dielectric having the dielectric constant of 7. The screen and keyboard parts are connected by two metallic hinges at the sides. The battery is modeled as a metal box with 1 mm plastic cover having a relative dielectric constant of 3. All shapes are maintained very close to the actual shapes (only very minor protrusions and rounded corners are not included), and all dimensions corresponded to the actual dimensions. Special consideration is given to model metal parts and connections between them accurately. Figure 5 gives two external views of the device under test. It should be noted that in Fig. 5 (a) the plastic plastic case of the bottom part and the dielectric cover of the battery are removed. Metals are shown in gray, keyboard in red and dielectric material with $\varepsilon = 3$ in yellow.

- The antenna is modeled as two lumped elements (capacitance and inductance) connecting the antenna to the 50 Ω source, a copper strip printed on a dielectric with ε=4.3 as the bottom part connected by a metal cylinder to the top wire of a diameter of 1.8 mm, and a metallic cup on top of the wire. Two positions of the antenna are modeled: fully extended and retracted.

SAR Computation, Procedures and Results

- Power level used for SAR normalization is 0.6 W, as specified by the manufacturer.
- Test configuration: as shown in Fig.1, with two antenna positions, as shown in Fig. 5.
- Computations are performed for the head placed as close to the screen of the computer as practically reasonable for an extremely shortsighted person, as illustrated in Fig. 1. This position results in the separation of the eyes from the screen of 15.5 cm. The head is centered with respect to the screen, and its closest separation to the antenna is 8.5 cm. The head is slightly tilted to more accurately reflect a real position. The neck and torso are not included, as it has been indicated by other researchers in their published papers that the error associated with such model truncation is negligible.
- Time averaging: not used.
- Summary of the results is given in Table 3, showing the head average SAR, peak 1g average SAR, coordinates for the peak SAR and gradient around the peak. The averaging is done only over the head mass that is shown in Fig. 1.

- The location of the peak SAR is done by an automatic search of the maximum voxel SAR.

Figures 6 and 7 show the head cross-sections with the voxel peak SAR, which also corresponds to the location of peak 1 g SAR, for the extended and retracted antenna, respectively. Figures 8 and 9 further illustrate the position of peak SARs, as they show contours of SAR greater or equal to 0.3 W/kg, for the two antenna positions, respectively. These figures also provide the rational explanation for a large gradient in x direction, which is due to the proximity of the peak SAR to the tissue-air interface. The location of the peak SAR is not unreasonable in view of the reflections from the bottom and screen parts of the computer that form a corner reflector. Additionally, a pseudo corner reflector appears to be formed by the nose-upper lip anatomy of the head. It should be noted that the second volume of SARs greater or equal to 0.3 W/kg is associated with smaller 1 g SAR than the principal volume for which data are givan in table 3.

Table 3. Summary of the computed results; 837 MHz, 600 mW output power

Antenna Position	Extended	Retracted
Head Ave SAR (W/kg)	0.015	0.017
Peak 1 g SAR (W/kg)	0.438	0.52
Peak SAR coordinates (mm)	207 x 121 x 113	207 x 121 x 113
Gradient [W/(kgm)]	108 $\mathbf{a}_x$ - 2.5 $\mathbf{a}_y$	129.3 $\mathbf{a}_x$ - 15.5 $\mathbf{a}_z$

- SAR 1 gram averaging procedure is done as follows:

The electric field components in each voxel are interpolated to the voxel center, i. e. the total field used to compute voxel SAR is based on 12 field components. A special algorithm is used to compute 1 g SARs, that is based on a low pass adaptive 3D spatial filter, as illustrated in Fig. 5. The filter has a cube shaped mask, that changes its volume via an adoption mechanism responding to changes in the density of tissue. In the design of the filter it is assumed that within one voxel, the mass and absorbed power are uniformly distributed. In general, the cube volume of the required mass comprises a number of full voxels in its core, and fractions of voxels in its outermost layer. For the case of a uniform mesh used, the algorithm to compute the averaged SAR in a SAR sampling point (X in Fig. 6) proceeds as follows:

- A sequence of cubes of increasing size (single voxel, 3 x 3 x 3, 5 x 5 x 5, etc.) is built by adding a layer of voxels to the previous cube until its mass is equal or larger than the required mass. In each expansion step it is verified that at least one voxel with tissue is present on every face of the new layer and that inside the cube the percentage of empty voxels does not exceed a preset value (typically 5%). If this is not satisfied, the SAR is considered indeterminate and the algorithm proceeds to the next SAR sampling point. The last cube in the sequence with a mass less than required is considered the *core* of the sought cubic volume.
- A cubic equation is solved to compute the fraction $f = dx/\Delta x$ of the additional layer that needs to be added to the core in order to obtain the required averaging mass. This equation is $cf^3 + ef^2 + sf - k = 0$, where c is the total mass of 8 corners, e is the total mass of 12 edges, s is the total mass of 6 sides, $f = dx/\Delta x$, and k is the required fraction of the outer layer mass.
- The power of core elements and weighted power contributions of the sides, edges and corners are added using appropriate powers of f as weights. SAR is computed by dividing thus obtained total power by the required mass.

References

J. Anderson, M. Okoniewski and S. S. Stuchly, “Practical 3D contour/staircase treatment of metals in FDTD”, *IEEE Microwave & Guided Wave Letters,* 6, no. 3, 1996.

K. Caputa, M. Okoniewski, and M. A. Stuchly, “An algorithm for computations of the power deposition in human tissue”, *IEEE Trans. Electromag. Compat.,* submitted for publication, 1998.

A. Taflove, “Computational Electrodynamics: The Finite-Difference Time-Domain Method”, Artech House Publications, 1995.

I. G. Zubal, C. R. Harrell, E. O. Smith, Z Rattner, G. R. Gindi, and P. H. Hoffer, “Computerized three-dimensional segmented human anatomy”, *Med. Phys. Biol.*, vol. 21, pp. 299-302, 1994.

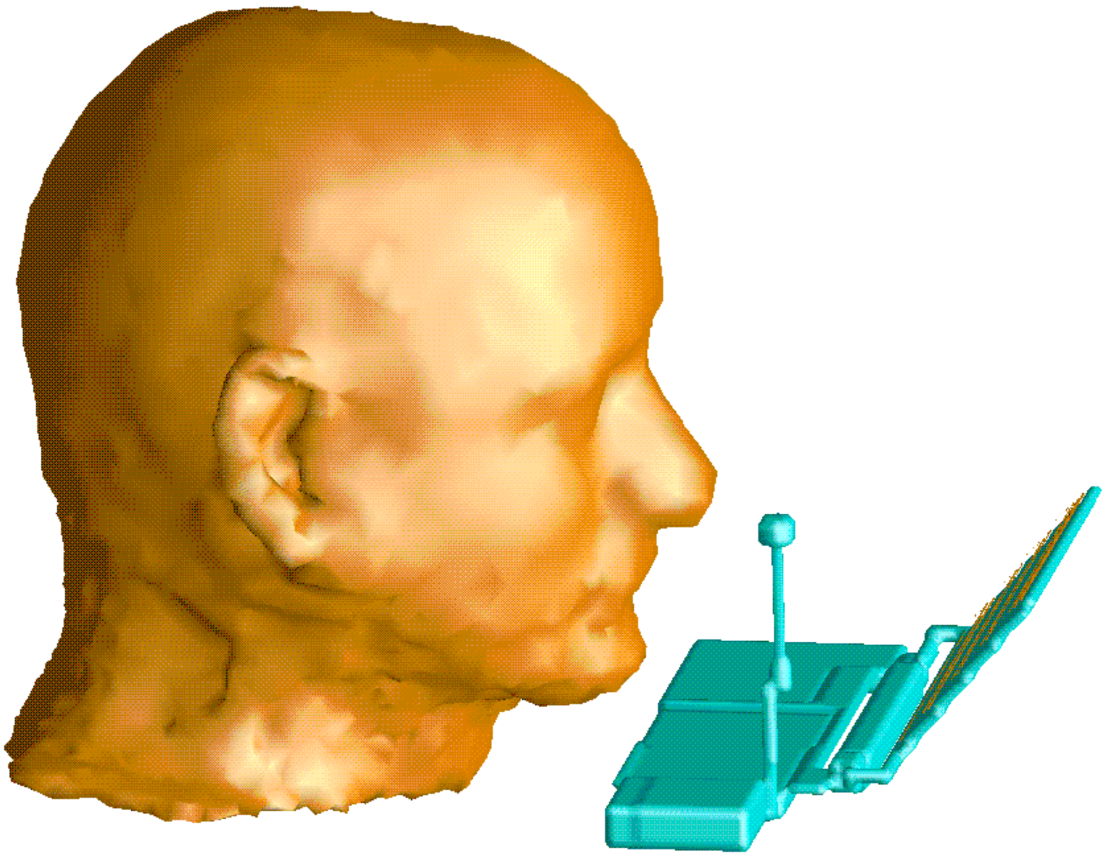

Figure 1: Illustration of the test device and head model. Note that the models are rendered, thus some distortions of the dimensions occur, most notably of the antenna.

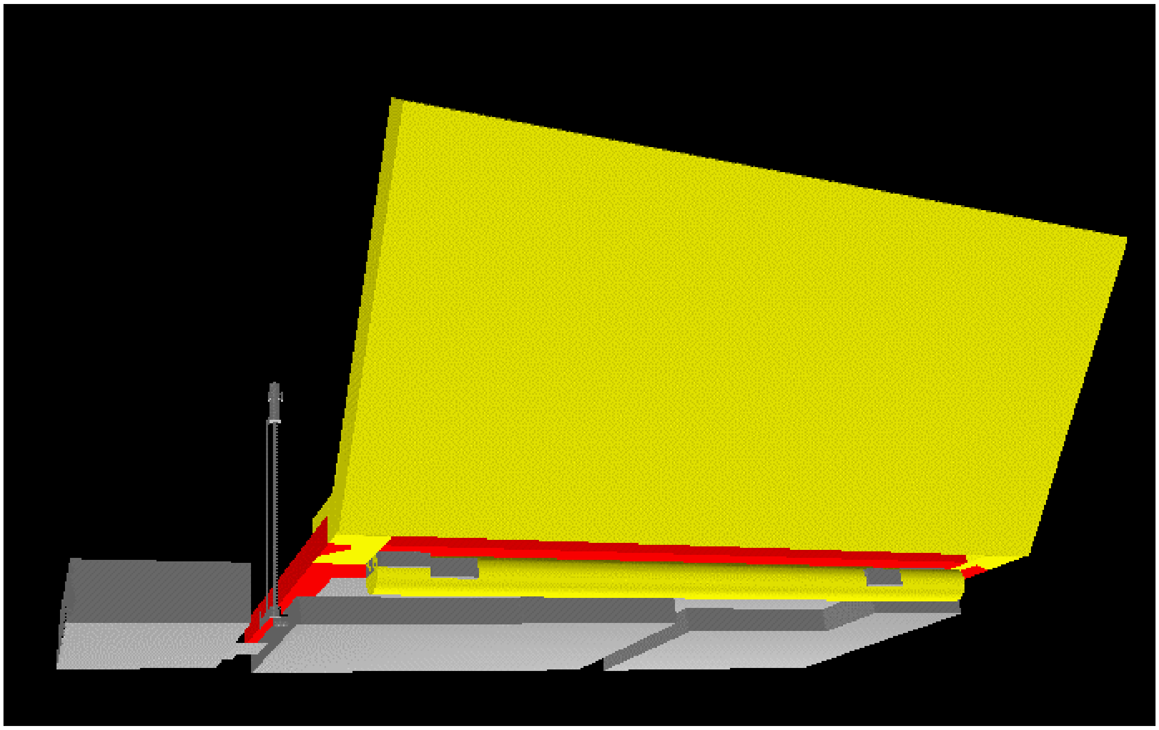

(a)

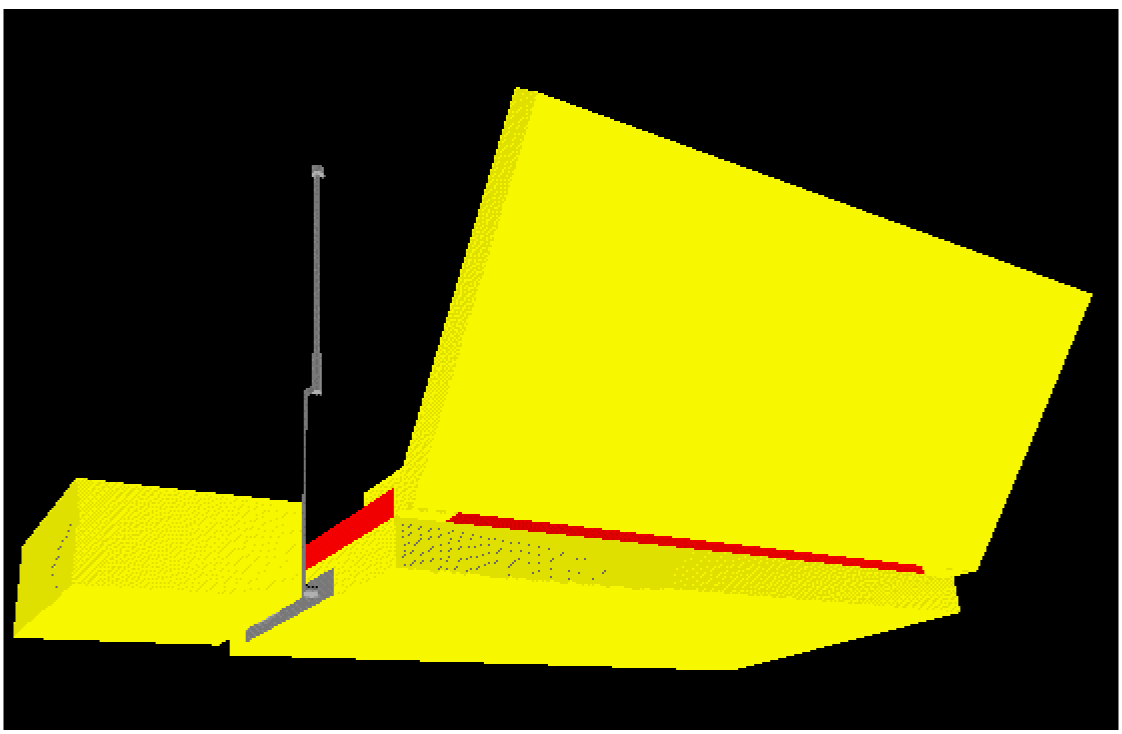

(b)

Figure 2: Test device model (a) antenna retracted, dielectric covers removed from the battery and the bottom part of the computer, and (b) antenna extended. Note that the colour coding is: metal – gray, dielectric covers – yellow, keyboard – red.

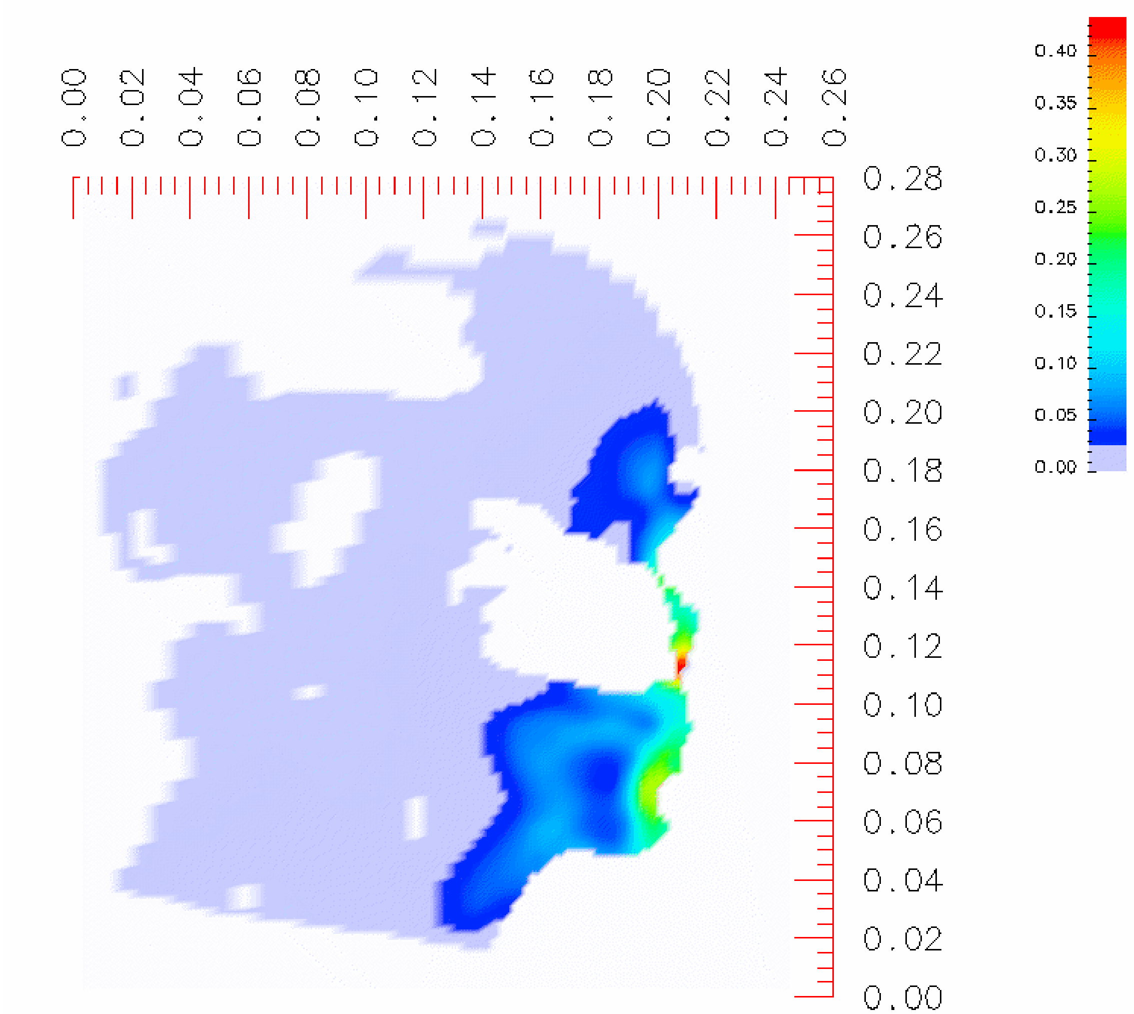

Figure 3: Cross section of the head in xz plane showing the location of peak 1g averaged SAR; antenna extended.

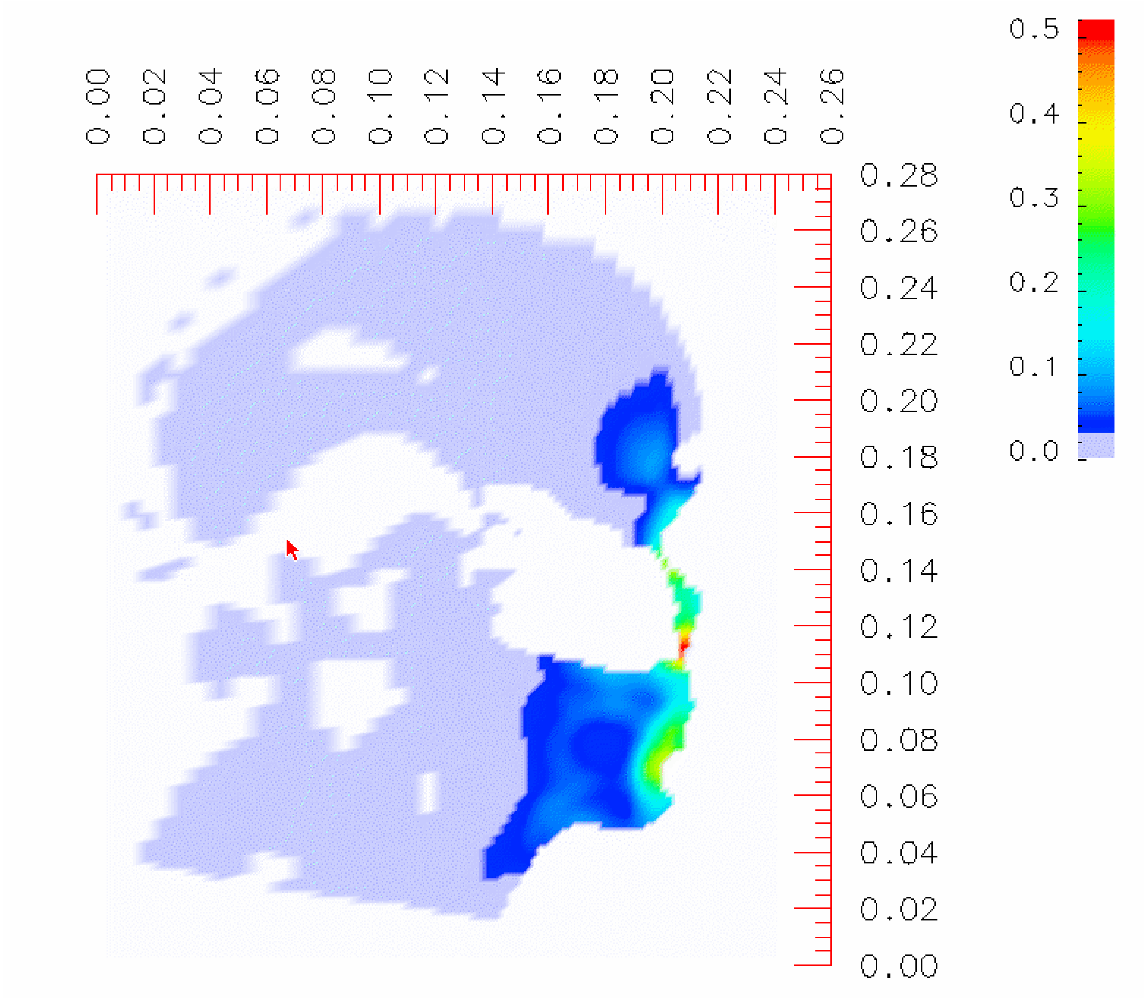

Figure 4: Cross section of the head in xz plane showing the location of peak 1g averaged SAR; antenna retracted.

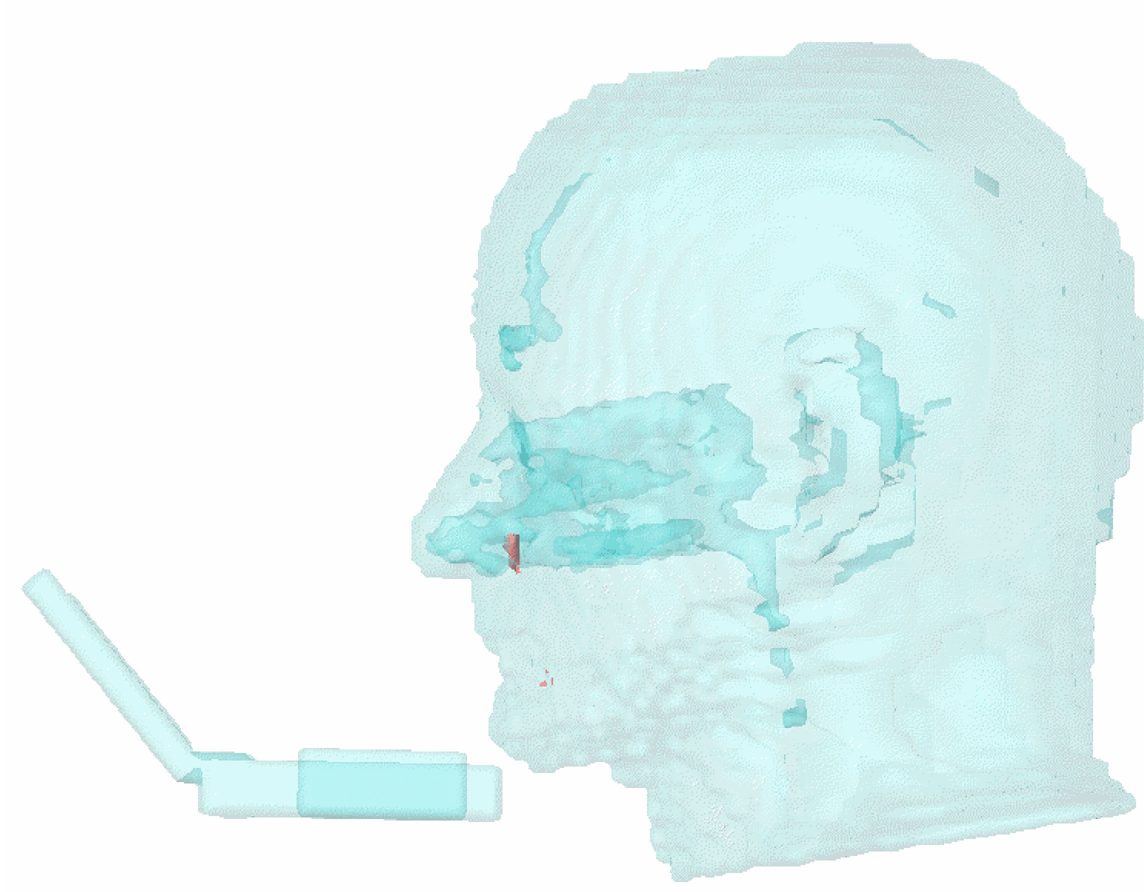

Figure 5: Location of volumes with SAR greater or equal to 0.3 W/kg (shown in pink), antenna extended.

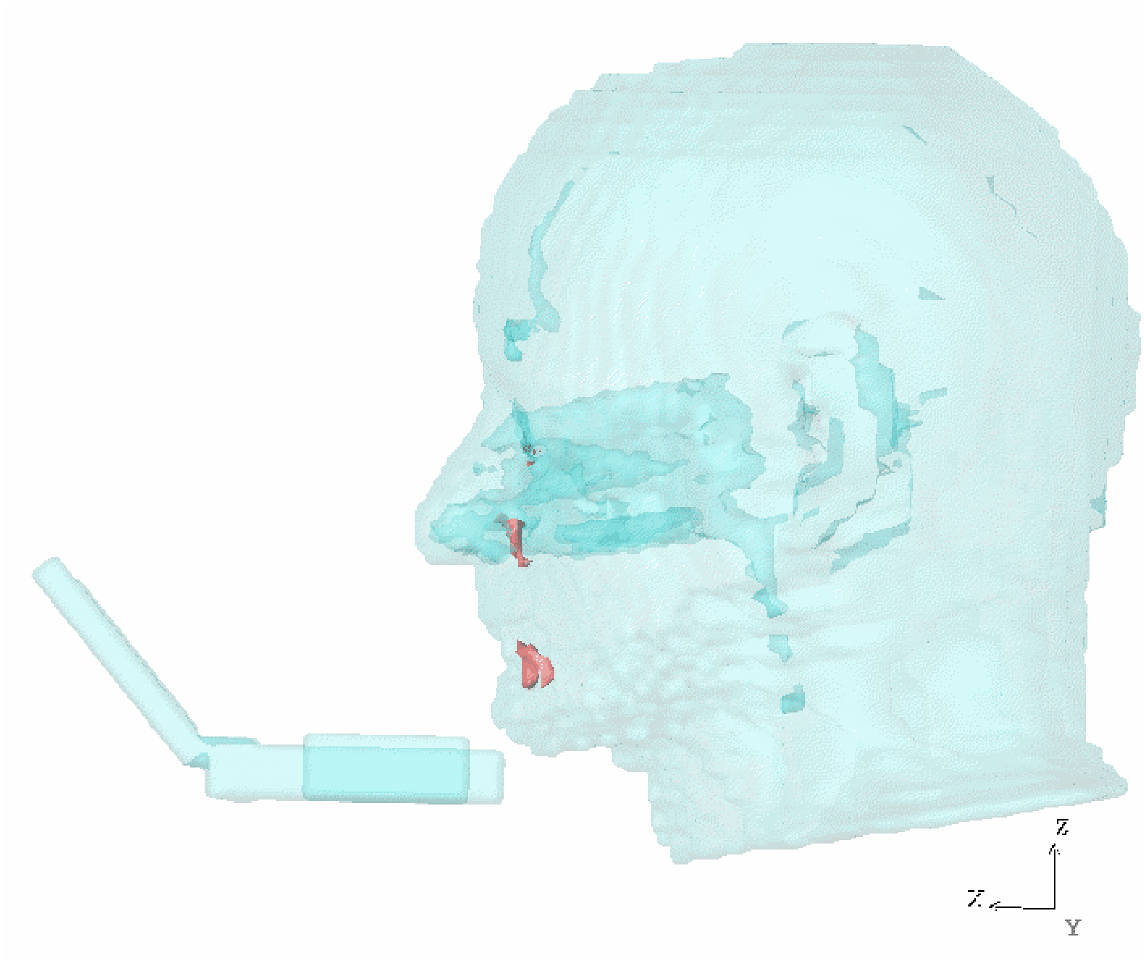

Figure 6: Location of volumes with SAR greater or equal to 0.3 W/kg (shown in pink), antenna retracted.

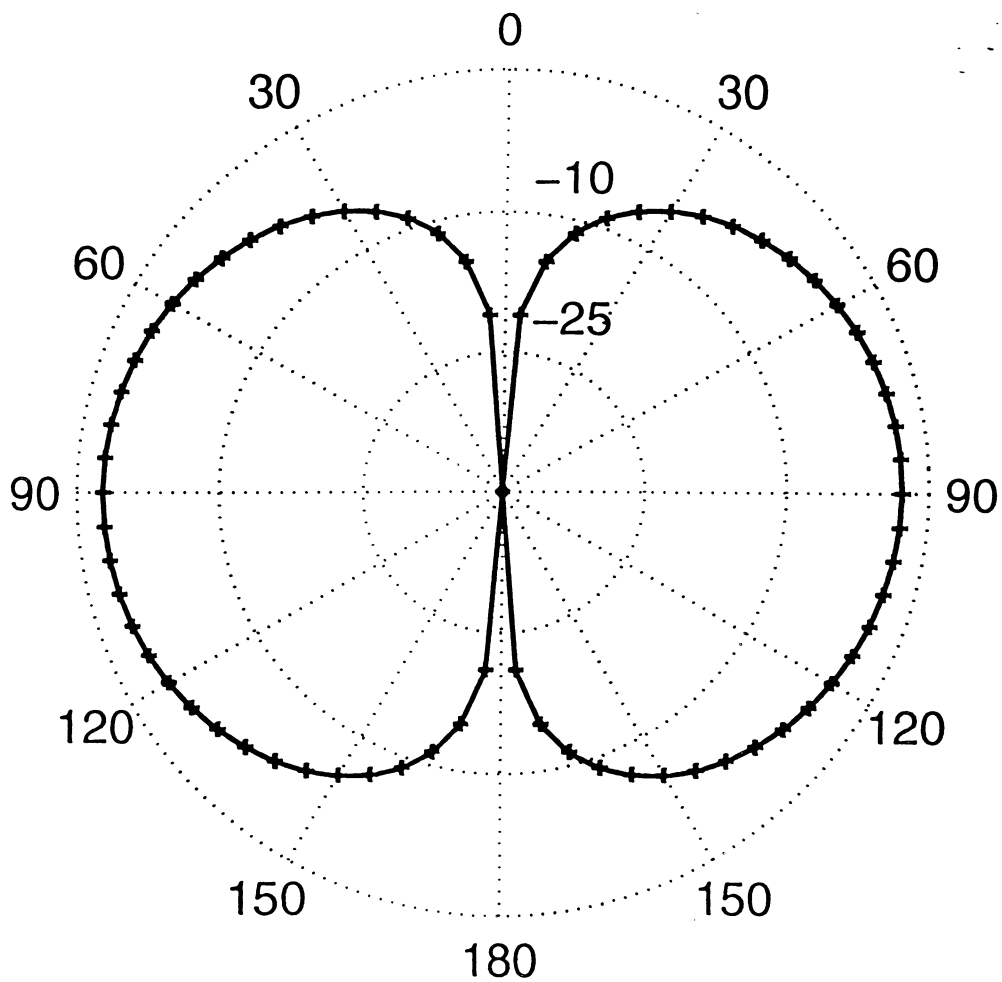

Figure 7: Far-field radiation pattern for a resonant dipole at 836 MHz; solid line - FDTD results, crosses – the NEC results.

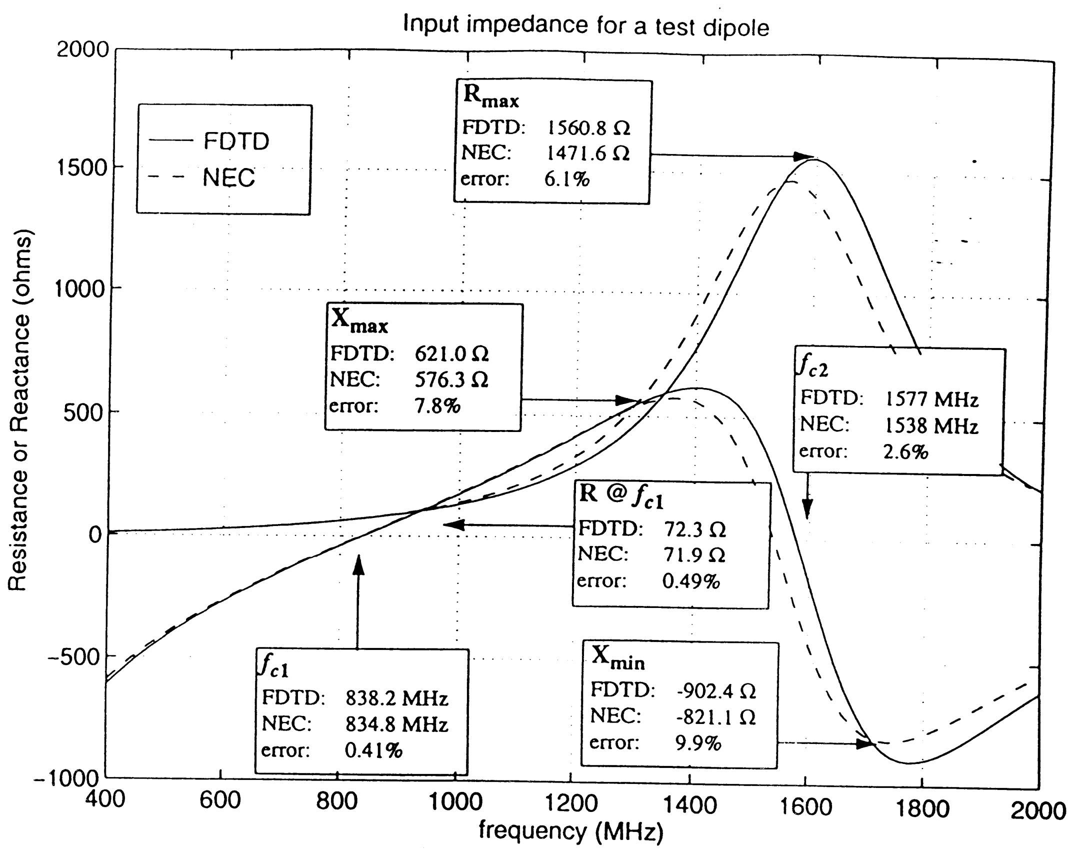

Figure 8: Input impedance of the test dipole; solid line – FDTD results, dashed line – NEC results.

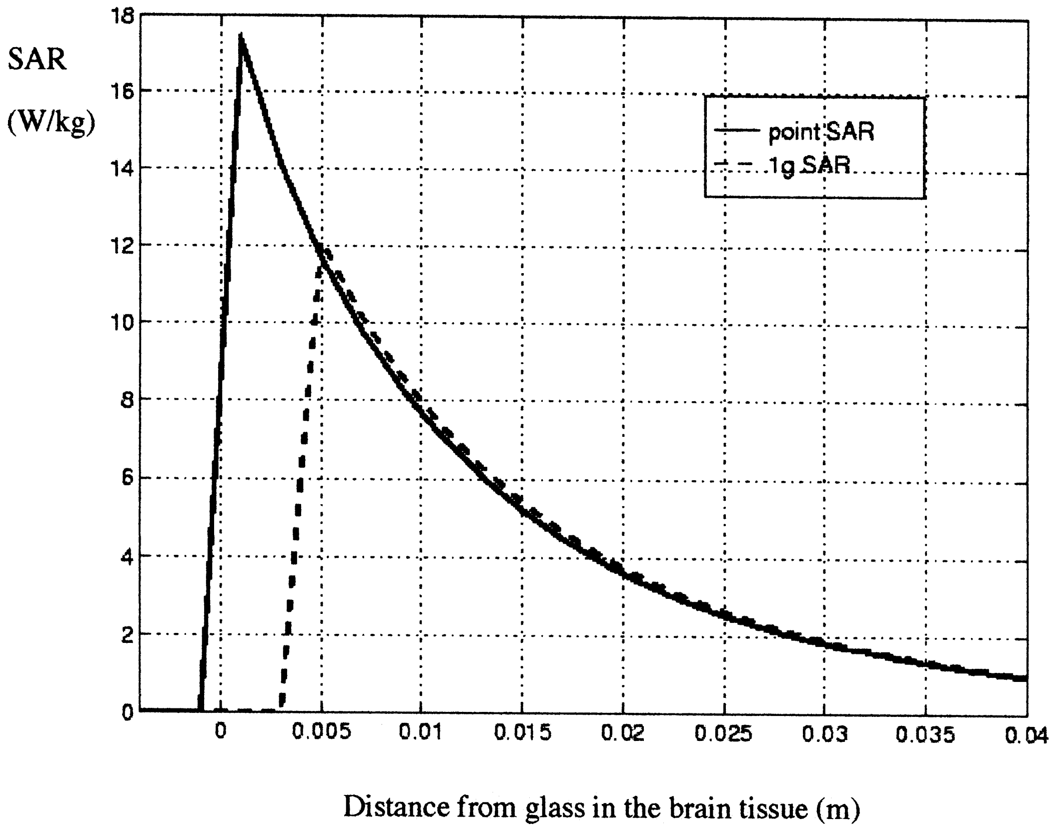

Figure 9: Voxel SAR (solid line), and 1g SAR (dashed line) at 0.84 GHz, output power of the antenna 1 W.

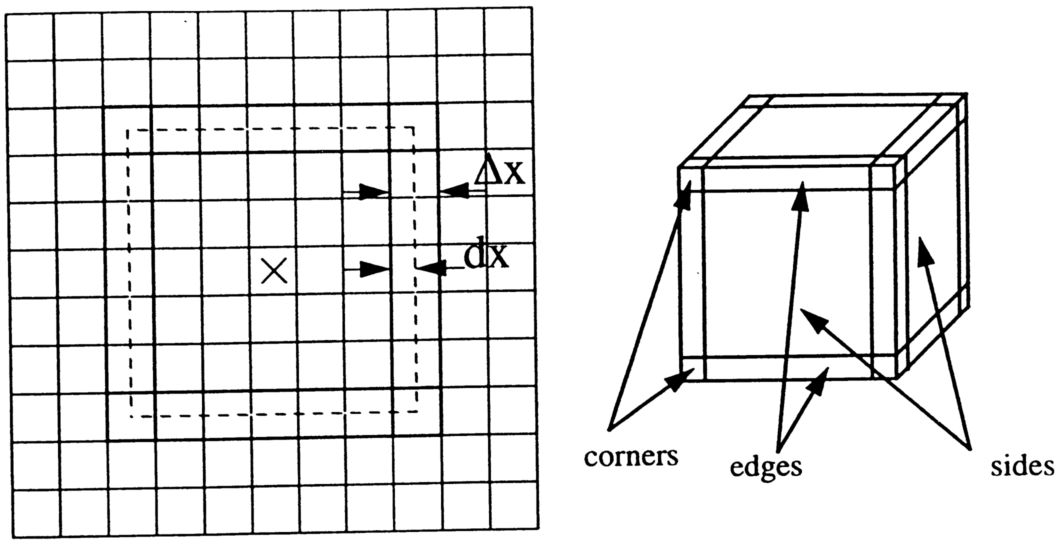

Figure 10: Mass-averaged SAR algorithm, construction of the core, and the cube of the specifies mass.